New Journal of Physics
The open access journal at the forefront of physics

Deutsche Physikalische Gesellschaft DPG IOP Institute of Physics

PAPER • OPEN ACCESS

Community lockdowns in social networks hardly mitigate epidemic spreading

To cite this article: Marko Gosak *et al* 2021 *New J. Phys.* **23** 043039

View the article online for updates and enhancements.

You may also like

- Reduction in human activity can enhance the urban heat island: insights from the COVID-19 lockdown
TC Chakraborty, Chandan Sarangi and Xuhui Lee
- Epidemic oscillations induced by social network control
Fabio Caccioli and Daniele De Martino
- The impact of the UK's COVID-19 lockdowns on energy demand and emissions
Daniel Mehlig, Helen ApSimon and Iain Staffell

This content was downloaded from IP address 102.90.43.132 on 23/04/2023 at 23:35

New Journal of Physics
The open access journal at the forefront of physics

Deutsche Physikalische Gesellschaft DPG
IOP Institute of Physics

Published in partnership with: Deutsche Physikalische Gesellschaft and the Institute of Physics

OPEN ACCESS

RECEIVED
3 January 2021

REVISED
18 March 2021

ACCEPTED FOR PUBLICATION
1 April 2021

PUBLISHED
20 April 2021

Original content from this work may be used under the terms of the Creative Commons Attribution 4.0 licence.

Any further distribution of this work must maintain attribution to the author(s) and the title of the work, journal citation and DOI.

PAPER

Community lockdowns in social networks hardly mitigate epidemic spreading

Marko Gosak[1,2], **Maja Duh**[1], **Rene Markovič**[1,3] **and Matjaž Perc**[1,4,5,*]

[1] Faculty of Natural Sciences and Mathematics, University of Maribor, Koroška 160, 2000 Maribor, Slovenia
[2] Faculty of Medicine, University of Maribor, Taborska 8, 2000 Maribor, Slovenia
[3] Faculty of Electrical Engineering and Computer Science, University of Maribor, Koroška 46, 2000 Maribor, Slovenia
[4] Department of Medical Research, China Medical University Hospital, China Medical University, Taichung, Taiwan
[5] Complexity Science Hub Vienna, Josefstädterstraße 39, 1080 Vienna, Austria
[*] Author to whom any correspondence should be addressed.

E-mail: matjaz.perc@gmail.com

Keywords: complex system, social network, epidemics, communities, cooperation, lockdown

Supplementary material for this article is available online

Abstract

Community lockdowns and travel restrictions are commonly employed to decelerate epidemic spreading. We here use a stochastic susceptible-infectious-recovered model on different social networks to determine when and to what degree such lockdowns are likely to be effective. Our research shows that community lockdowns are effective only if the links outside of the communities are virtually completely sealed off. The benefits of targeting specifically these links, as opposed to links uniformly at random across the whole network, are inferable only beyond 90% lockdown effectiveness. And even then the peak of the infected curve decreases by only 20% and its onset is delayed by a factor of 1.5. This holds for static and temporal social networks, regardless of their size and structural particularities. Networks derived from cell phone location data and online location-based social platforms yield the same results as a large family of hyperbolic geometric network models where characteristic path lengths, clustering, and community structure can be arbitrarily adjusted. The complex connectedness of modern human societies, which enables the ease of global communication and the lightning speeds at which news and information spread, thus makes it very difficult to halt epidemic spreading with top-down measures. We therefore emphasize the outstanding importance of endogenous self-isolation and social distancing for successfully arresting epidemic spreading.

1. Introduction

The structure of social networks critically affects epidemic spreading [1, 2]. Research has shown that properties that are universally associated with social networks, such as small characteristic path lengths, high clustering [3], and broad-scale degree distributions [4], often work together to provide an environment where epidemics spread fast and virtually uninhibited across the population [5–11]. This spreading is often accelerated further by the temporal component of social networks [12], where traveling and mobility, in particular, play an important role [13–20]. Furthermore, social networks exhibit strong community structure [21], which has not only proven to importantly and in a non-trivial way affect the epidemic spreading [22–26], but has also implications for how networks can be protected from major outbreaks [27].

However, the structure of social networks also affects many other aspects of our behavior, especially how we interact and perceive others. We do not simply strive to amass the greatest amounts of conveniences with the least possible effort as 'economic man' would, but because we are connected to others in intricate ways, we often sideline our inherent self-interest and take their wellbeing into account as 'network man' would

© 2021 The Author(s). Published by IOP Publishing Ltd on behalf of the Institute of Physics and Deutsche Physikalische Gesellschaft

[28, 29]. This decelerates epidemic spreading, for example because we self-isolate [30, 31] and because we vaccinate [32–35], even though both actions are costly to us but benefit others. In other words, we cooperate [36–39], which at such a large scale and among non-kin is almost unique to humans.

In addition to endogenous bottom-up measures that can halt epidemic spreading, one of the most commonly adopted institutional top-down measures is to impose community lockdowns. This can range from isolating a couple of infected individuals to locking down entire neighborhoods or even whole cities, as done recently in response to the COVID-19 pandemic [40]. Arguably, such measures can be effective in significantly decelerating epidemic spreading, for example rendering an initial exponential growth of cases subexponential [41]. On the other hand, they are often difficult and costly to implement [42, 43], and they carry with them adverse side effects that can sometimes outweigh the benefits [44].

The question that we here seek to answer is, when exactly do community lockdowns work, and which conditions need to be fulfilled, both in terms of the structure of the social network and in terms of the severity of the lockdowns, to achieve a significant positive impact in terms of mitigating epidemic spreading. To that effect, we use a stochastic susceptible-infectious-recovered model that we simulate on random geometric graphs in hyperbolic spaces, which yield networks that have heterogeneous degree distributions, strong clustering, short average path lengths, and community structure, which are all inherent properties of real social networks [45, 46]. We also use a static as well as a dynamic version of an empirical social network obtained from cell phone location data, to corroborate the robustness of our results.

In what follows, we will show that community lockdowns hardly mitigate epidemic spreading. In particular, they do so only if the lockdowns of communities are really tight. Even a 10% lockdown ineffectiveness renders the community lockdown no more efficient than reducing the contact rates in the same extent uniformly across the whole network. This arguably has to do with the complex connectedness of modern human societies that can be seen in the ease of global communication, and in the lightning speeds at which news and information as well as epidemics and financial crises spread [29]. Nonetheless, it is still very surprising to see just how little it takes for the lockdowns to fail and for the epidemics to spill over between communities and eventually across the whole network. Our research thus prompts the emphasis of the outstanding importance of endogenous self-isolation and social distancing for effectively halting epidemics. Top-down measures, such as community lockdowns, are at beast just a proxy by means of which decision-makers can hope to reduce social contacts, but on their own they fail to significantly decelerate epidemic spreading.

2. Mathematical model and networks

To study the effectiveness of community lockdowns in halting epidemic spreading, we simulate a stochastic susceptible-infectious-recovered model on different social networks. Random geometric graphs in hyperbolic spaces have properties that are commonly observed in real social networks, such as a heterogeneous degree distribution, small diameter, strong clustering, and the presence of communities [45–48]. To generate a geometric graph in a hyperbolic space we start with $n = 5$ connected nodes and then add new nodes i that are mapped onto a hyperbolic disc with randomly assigned polar coordinates

$$\theta_i = 2\pi u_1, \tag{1}$$

$$r_i = \frac{1}{\alpha}\cos^{-1}\left[1 + \cosh(\alpha R_{\mathrm{h}} - 1)u_2\right]. \tag{2}$$

Here α is the internal growth parameter, R_{h} is the radius of the hyperbolic disc, and u_1 and u_2 are random numbers sampled from a $[0, 1]$ uniform distribution. The polar coordinates r_i and θ_i correspond to the popularity and similarity of a node i, respectively. Moreover, the spatial positions of nodes in the hyperbolic space can reflect actual properties of a real social network. For example, nodes that are close to each other in the hyperbolic space correspond to individuals that live in the same geographic region, or belong to the same geo-political or economic group [49, 50].

Each time a new node i is added, it is connected to the existing nodes with a probability that is proportional to the hyperbolic distance d_{ij} between the new ith and the existing jth node. This probability is determined according to

$$d_{ij} = \cosh^{-1}[\cosh(r_i)\cosh(r_j) - \sinh(r_i)\sinh(r_j)\cos(\triangle\theta_{ij})], \tag{3}$$

where $\triangle\theta_{ij} = \pi - |\pi - |\theta_i - \theta_j||$ is the angular distance between the ith and the jth node. In our simulations, we use parameter values $\alpha = 0.15$, $R_{\mathrm{h}} = 10$, $\langle k\rangle = 10$ and a network with 10^5 nodes, which yields paradigmatic social networks, as shown in [45–47].

Specifically, the resulting network is characterized by a broad-scale degree distribution, a positive assortativity coefficient (0.25), high modularity ($Q = 0.84$), and small-world characteristics. The later are reflected by a high clustering coefficient ($C_{\mathrm{avg}} = 0.55$) and a short average path length ($L_{\mathrm{avg}} = 7.3$), which yields a high value of the small-worldness parameter ($sw = 7.0 \gg 1$) [51]. Due to these genuine topological characteristics, the hyperbolic network model represents a viable platform for simulating various social phenomena, including epidemics [48, 52, 53].

We also use a real social network, obtained from jointly considering cell phone location data and data from two online location-based social platforms, which consists of 58 228 nodes and 214 078 edges [54]. In addition to the static social network structure with aggregated interactions, we also consider a temporal network of contacts between individuals, as obtained with the same dataset. We use a period of 200 consecutive days, with social interactions assembled on a weekly basis.

To detect communities in these networks we use a modularity-based optimization method [21, 55], where the modularity

$$Q = \frac{1}{2m}\sum_{i,j}^{N}\left[A_{ij} - \frac{k_i k_j}{2m}\right]\delta(c_i, c_j) \tag{4}$$

determines how well a network can be the partitioned into communities [56]. Here m is the total number of edges in the network, k_i and k_j are the degrees of nodes i and j, c_i and c_j are membership variables that assigns nodes i and j to a specific community, and $\delta(c_i, c_j)$ is a delta function that is equal to 1 if $c_i = c_j$ and 0 otherwise. The algorithm seeks to find the most likely community structure of the network by repeatedly partitioning nodes into different communities until the modularity is maximized.

The stochastic susceptible-infectious-recovered model is defined as follows. Each node can be either in the susceptible (S), infectious (I), or recovered (R) state. The exposed or non-exposed state depends on the contact rates an individual has with others (see below). Initially, we select 1% of the nodes in one community uniformly at random and designate them as infected (I). The remaining 99% of the nodes in the randomly selected infected community and all the nodes in other non-infected communities are designated as susceptible (S). We assign a contact rate q_{ij} to every pair of nodes i and j, where $q_{ij} = 0$ means that the given pair will not interact and that thus the disease cannot spread between them. If a node i has $q_{ij} = 0$ for all j it is non-exposed. At the other extreme, $q_{ij} = 1$ corresponds to an unaltered probability for the transmission of the infection. We note that $q_{ij} < 1$ can also be interpreted as social distancing or mobility impairment. We consider two cases in our research: (i) the contact rate is reduced uniformly for all nodes such that $q_{ij} = q_{\mathrm{a}}$, where q_{a} is the average mobility, and (ii) only the contact rates between nodes from different communities are decreased. The extent of the later measure is defined with the between-community immobilization parameter $p \in [0, 1]$ such that

$$q_{ij} = \begin{cases} q_{\mathrm{a}}; & \text{if } c_i = c_j \\ q_{\mathrm{a}}(1-p); & \text{if } c_i \neq c_j \end{cases} . \tag{5}$$

Thus, for $p = 0$ the between-community mobility is equal to the within-community mobility q_{a}, while for $p = 1$ interactions between nodes from different communities are not possible. For $p = 0.5$, for example, the rate of interactions between communities is 50% lower than it is within the communities.

We use the Monte Carlo method to simulate this stochastic susceptible-infectious-recovered model on social networks [57]. The method corresponds to random sequential updating, such that during a full Monte Carlo step (MCS) each node gets a chance once on average to become infected. Each full MCS consist of repeating the following elementary step n times. Firstly, we select a node i uniformly at random from the whole network. Secondly, (i) if node i is in state S, we choose one neighbor j uniformly at random and visit it with probability q_{ij}. If the neighbor is visited and is in state I, node i becomes infected with probability $w = 0.5$. If, however, the neighbor j is in states S or R nothing happens. (ii) If node i is in state I, we verify if at least $t_r = 15$ full MCS have passed since it became infected. If yes, node i becomes recovered (R), and if no, node i remains infected. (iii) If node i is in state R, nothing happens. All presented results are averages over 100 independent runs with different initial conditions for each set of parameters.

3. Results

We first show a series of snapshots of a hyperbolic geometric network that has properties that are commonly observed in real social networks over time in figure 1, where an epidemic unfolds as per the stochastic susceptible-infectious-recovered model. Initially only 1% of randomly chosen nodes in one randomly chosen community are infected (I), while all the other nodes are designated as susceptible (S).

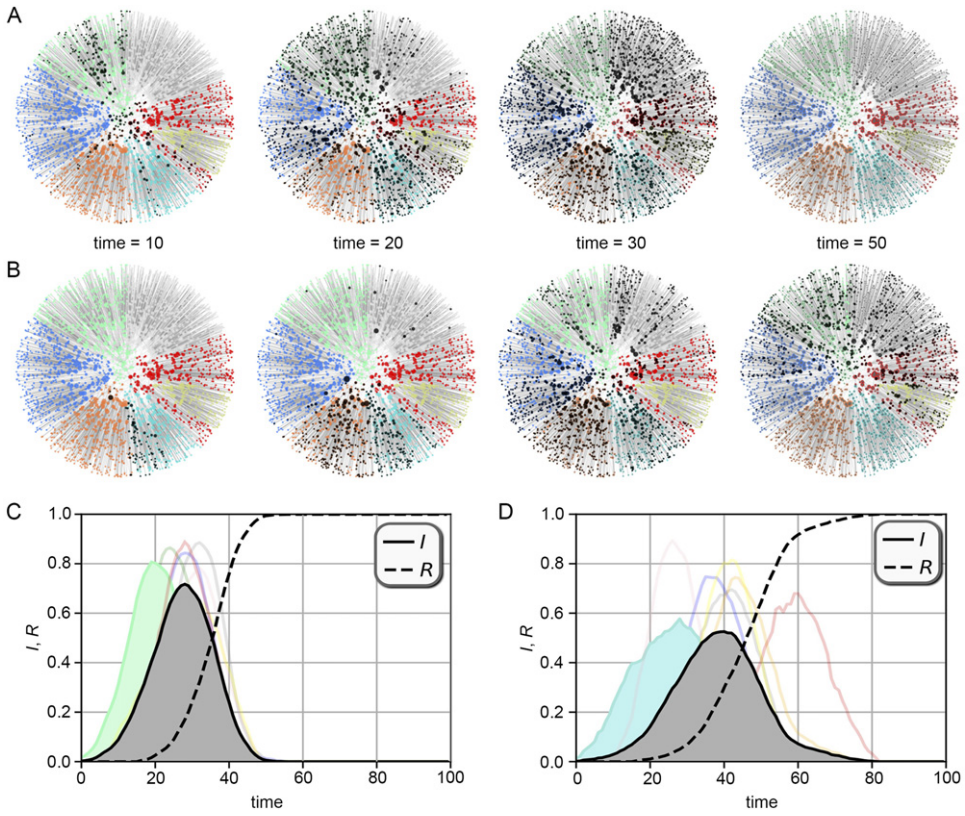

Figure 1. The evolution of the stochastic susceptible-infectious-recovered model on a hyperbolic geometric network with and without community lockdowns. (A) Epidemic spreading, presented as a sequence of network snapshots over time, as obtained without community lockdowns. (B) Epidemic spreading with a 90% reduced interaction rate between communities. Different node colors denote different communities. Later in time, infected nodes are colored black, while recovered nodes are overlaid with gray circles. Panels (C) and (D) show the corresponding fractions of infected I and recovered R individuals over time without and with the 90% community lockdown, respectively. The full black line shows the average value of infected individuals in the whole population, whereas the transparent colored lines indicate the fractions I within particular communities. The cyan curve with the shaded area shows results for the initially infected community. The dashed black line represents the fraction of recovered individuals in the entire network. We have used the average contact rate $q_a = 1.0$ for both cases, and a smaller network with only 3000 nodes for clarity. These results are also available as a movie in the supplementary video S1.

In (A) all the links are completely active, thus allowing the epidemic to spread uninhibited. In (B) all the links that connect the nodes of different communities are inhibited. Specifically, we apply a 90% reduced contact rate for the latter, which means that the between-community interactions are severely impaired. The 90% reduced contact rate can also be interpreted as strict social distancing or reduced mobility between different communities. By following the network snapshots from left to right, a faster course of the epidemic spreading can be observed in the upper panel. In the lower panel it can be observed that initially the infections indeed spread only within the initially infected community, but soon enough nearby communities become infected too. From there onwards the epidemic spreads progressively across the whole network. Even though the epidemic spreading is faster in the case without the community lockdown, the epidemic spreads across the whole network in both cases, thus indicating that constraining the interactions between all communities is only marginally effective in reducing disease transmission.

The limited effectiveness of the harsh community lockdown is further corroborated by the results shown below the network snapshots in figures 1(C) and (D), where the fraction of infected and recovered individuals is shown over time separately for both scenarios. It can be observed that the peak fraction of infected individuals decreases by 18%, from 74% to 56%, and the peak also occurs somewhat later in time. Put differently, the infected curve is flattened to some degree due to the lockdown, but the fraction of recovered individuals, which is essentially equal to the area under the infected curve, rises to 100% in both cases. Thus, even if the community lockdown is 90% effective, the infected curve is only marginally flattened due to delays in disease transmission between communities, while the total number of infected individuals is not affected at all. A more detailed view of how the epidemic spreads in both considered cases can be seen in supplementary videos S1 and S2 (http://stacks.iop.org/NJP/23/043039/mmedia), where animations of the epidemic spreading are presented for the hyperbolic network model and for an actual location-based social network [54], respectively.

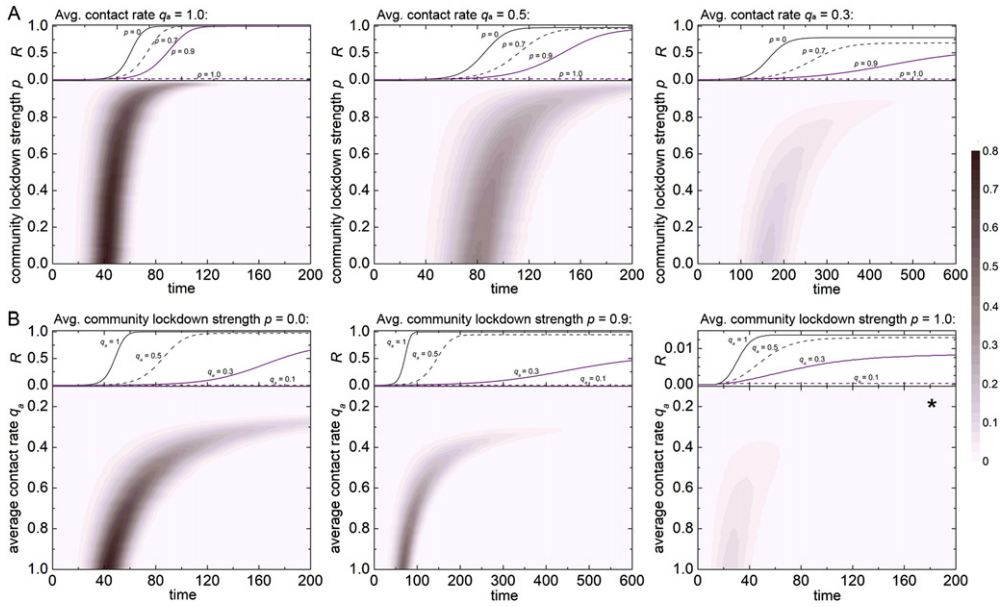

Figure 2. Quantitative impact of community lockdowns and social distancing. Color maps encode the fraction of infected individuals over time, while the corresponding top panels show the fraction of recovered individuals for representative values of the community lockdown strength p in (A) and of the average contact rate q_a in (B). Color maps in (A) show the impact of community lockdowns as obtained for different average contact rates from left to right, while color maps in (B) show the impact of different average contact rates as obtained for different community lockdowns from left to right. We note that the average contact rate can be interpreted as endogenous social distancing or mobility impairment, where $q_a = 1$ corresponds to no distancing or mobility impairment, while $q_a = 0$ would correspond to no personal contact at all, neither within nor between communities. The star in the rightmost panel of (B) indicates that the color scale is ten-fold smaller, i.e. from 0–0.08.

To study the effectiveness of community lockdowns more precisely, we show in figure 2 color maps of the fraction of infected individuals over time, as obtained for different combinations of the average contact rate q_a and the community lockdown strength p on a hyperbolic geometric network. In (A) the average contact rate decreases from 1 (fully active links) to 0.5 (only every second encounter results in a possible infection) and finally to 0.3, from left to right. Vertically, the community lockdown strength increases from 0 to 1. It can be observed that the community lockdown starts to show an effect only when it is above at least 80% effective, with beyond 90% showing a more noticeable positive impact. This holds for $q_a = 1$ and $q_a = 0.5$. If the average contact rate is lower, the community lockdown is somewhat more effective already at lower values of p, but this is a joint effect stemming for the combination of overall decreased mobility (or increase social distancing) enacted by $q_a \ll 1$ and community lockdowns. In fact, for $q_a = 0.3$ the epidemic is effectively halted even at $p = 0$, i.e. without any community lockdowns. The further corroborate this, we show in (B) results for three different community lockdown strengths, namely $p = 0$, $p = 0.9$ and $p = 1.0$, from left to right respectively. It can be observed that the epidemic can only be halted if a severe lockdown of communities ($p = 0.9$) is in addition accompanied by reduced personal interactions within communities, or if the communities are truly completely sealed off with $p = 1$.

The panels above the color maps show the corresponding fractions of recovered individuals over time, for characteristic values of p in the top three color maps and for characteristic values of q_a in the bottom three color maps. It can be observed that a noticeable decrease in the overall fraction of infected individuals (who eventually recover) is attainable only if diminished interactions among all communities are accompanied by ample social distancing or immobilization over the whole network ($q_a \ll 1$). Put differently, the effect of $q_a < 1$ is significantly more obvious than an increase of p up to 0.8, until which the impact of community lockdowns is barely inferable. Only beyond $p = 0.8$ does the community lockdown contribute to a notable mitigation of epidemic spreading. We thus have the conclusion that social distancing and immobilization across the whole population, even if only 50% effective ($q_a = 0.5$) is significantly more effective in halting epidemics, both in terms of flattening the curve and in terms of the total number of infected individuals, than even the harshest of community lockdowns at over 90% effectiveness.

An unanswered question remains, however, whether and to what degree the blocking of links between communities is more effective than if we simply reduce an equivalent extent of contact rates uniformly across the whole network. In figure 3 we show two series of plots, obtained for three different average contact rates q_a (full lines with symbols) and the corresponding decrease in overall contact rate (transparent lines with symbols), as obtained on random geometric graphs that model actual social networks (top row)

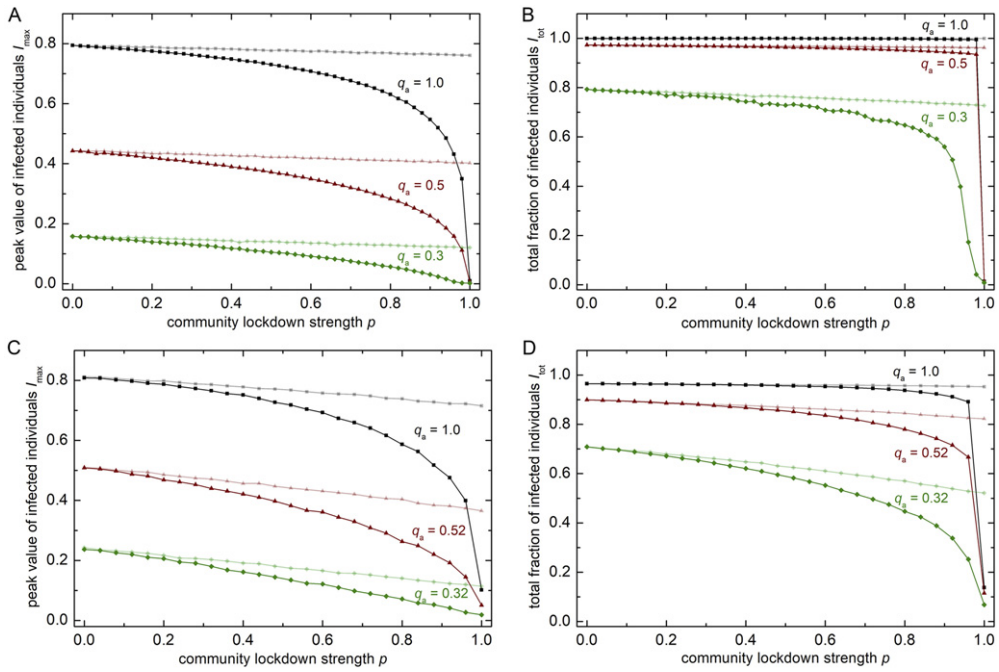

Figure 3. The peak impact of community lockdowns and social distancing on the epidemic curve. Peak values of infected individuals I_{max} (A) and (C) and the total fraction of infected individuals I_{tot} (B) and (D) as a function of reduced contact rates, as obtained on a hyperbolic geometric network (A) and (B) and on the empirical contact network (C) and (D). In each panel, full lines with symbols show the epidemic outcome as a function of the community lockdown strength p for different values of the average contact rate q_a, whereas the corresponding transparent lines with symbols show the epidemic outcome for an equivalent decrease in the overall contact rate q_a that precisely matches the decrease in between-community interactions. On both networks community lockdowns are only marginally effective in reducing either the peak value or the total number of infected individuals, unless the lockdown is very severe ($>90\%$ reduction in the between-community contact rate) or accompanied by rather strict social distancing, as obtained with a reduced average contact rate $q_a < 0.5$.

and on an actual location-based social network [54] (bottom row). In (A) and (C) we show peak values of infected individuals, while (B) and (D) we show the total fractions of infected individuals. Both series of plots tell the same story, namely that targeting and shutting down links between communities has only marginally better prognosis for halting the epidemic than reducing interactions uniformly across the whole network. Unless the community lockdown is very severe ($>90\%$), the peak values and total fractions of infected individuals are hardly reduced if the interactions within communities remain unaltered ($q_a = 1$). If, however, the links within the communities are also impaired by decreasing the average contact rate, then targeting between-community links is noticeably more effective than immobilizing interactions uniformly at random across the whole network. But it is important to note that we are in this case again witnessing the combined effect of social distancing (enacted through an overall decreased contact rate) and community lockdown.

We also explore the impact of community lockdowns on epidemic spreading in a temporal social network. For this, we map the location-based social network [54] onto time-ordered lists, so that we obtain the nodes, the interactions between them, and the corresponding community indices for 200 consecutive days. The temporal network of social interactions is thus a sequence of adjacency matrices, wherein the evolution is described by the appearance and disappearance of nodes and edges over time. The simulation of epidemic spreading over dynamic contacts is conceptually very similar as for static networks. During a full Monte Carlo step, each node is selected once on average, and can get infected from current neighbors with probability w, whereby the states of all nodes (S, I, E) are transmitted across successive days.

Figure 4 shows the results obtained for the temporal social network. The color map in (A) shows the evolution of the epidemic for different community lockdown strengths, with no lockdown at the bottom and full lockdown at the top. The upper panel shows how the fraction of recovered individuals varies over time for three representative community lockdown strengths. In comparison with the results obtained for the static social network, the epidemic spreading is less coherent, spans over a broader time interval, exhibits multiple minor peaks in the number of infected individuals, and only approximately half of the nodes gets infected. These observations go well in hand with previous reports on epidemic spreading in temporal networks, and they must be attributed to comparable timescales of the contact and the infection dynamics, which also confines the contagion flow due to the presence of temporally impossible paths

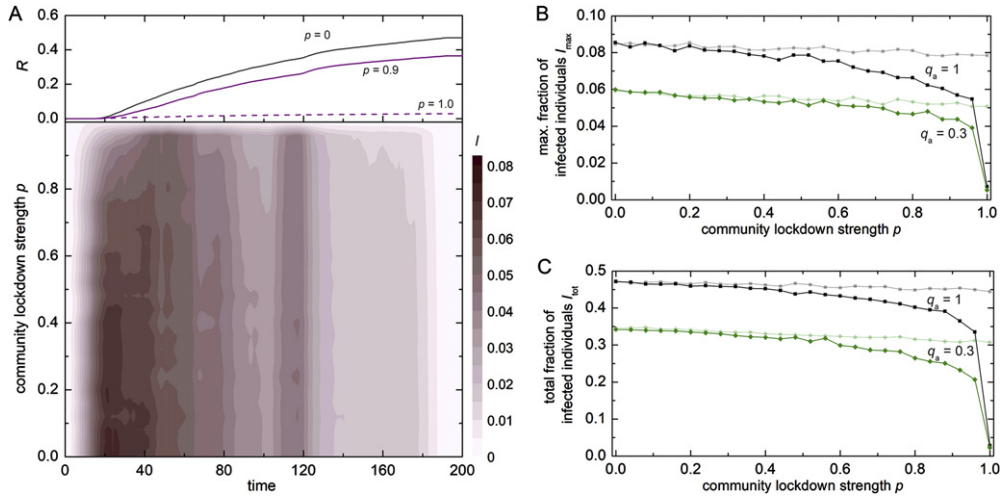

Figure 4. The impact of community lockdowns on epidemic spreading in a real temporal contact network. (A) The evolution of the epidemics as a function of community lockdown strength p. The fraction of infected individuals I is color-coded, while the fraction of recovered individuals R is shown in the top panel for three characteristic values of the community lockdown strength p. In the simulation, we have used the average contact rate $q_a = 1.0$. (B) Peak values of infected individuals I_{max} in dependence on the community lockdown strength p, as obtained for different values of q_a. (C) Total fraction of infected individuals I_{tot} in dependence on the community lockdown strength p, as obtained for different values of q_a. In (B) and (C) the transparent lines show the outcome of the epidemic for an equivalent decrease in overall contact rate q_a that corresponds precisely to the decrease in between-community interactions.

[1, 58]. However, despite of these differences that are due to the time-varying interactions, the obtained results in terms of the effects of community lockdowns are very similar to those we have reported above for static networks. Indeed, only very high levels ($>80\%$) of community lockdown contribute effectively to the mitigation of epidemic spreading. The inefficiency of community lockdowns to halt epidemic spreading on temporal social networks is further corroborated by the results presented in (B) and (C), where the peak and total values of infected individuals are presented, in comparison to what we would obtain if we simply decreased the average contact rate without paying attention to between-community links. It can be observed that the targeted weakening of links that connect nodes from different communities only marginally outperforms the proportional homogeneous reduction of contact rates across the whole network.

Taken together, results in figures 3 and 4 clearly show that community lockdowns in social networks hardly mitigate epidemic spreading, or they do so only marginally better than the homogeneous reduction of contact rates across the whole network. The details of this conclusion are robust to variations in network structure, holding as much for a large class of artificially generated hyperbolic geometric networks that have properties akin to real social networks, as they do on actual real-life static as well as temporal social networks created from cell phone location data and online location-based social platforms.

4. Discussion

We have shown that community lockdowns in social networks hardly mitigate epidemic spreading. In the best case scenario, when the links between all communities are virtually entirely locked down right from the start, we can hope to flatten the infected curve by decreasing the peak by about 20% and by delaying its onset by a factor of 1.5–2, for example from 20 to around 40 days, both compared to none containment measures being taken at all. A detailed analysis of the effect of community lockdowns on epidemic spreading reveals that they are more effective if they are implemented jointly with social distancing across the whole social network. In such a case a high-quality lockdown is likely to be more effective, in particular not only flattening the infected curve and prolonging the peak time, but also decreasing the total number of infected individuals that will be affected by an epidemic. On the other hand, however, our research also shows that the very same effects are attainable without community lockdowns, simply by implementing more stringent social distancing or mobility restrictions. The conclusion is that top-down approaches aimed at mitigating epidemic spreading, such as community lockdowns, come in second-best behind bottom-up endogenous self-isolation and social distancing. And what is more, the former work really poorly in the absence of the latter. Notably, these findings go well in hand with what was observed in recent studies about

the effects of non-pharmaceutical interventions on COVID-19 transmission [59–63], as we discuss in more detail in what follows.

In our study, we have utilized a paradigmatic SIR compartmental model, which provides a very simple framework to study transmission dynamics of infectious diseases. As such, it allows for an intuitive exploration of how epidemics unfold, and has been either in its basic or modified form often used to simulate also the spread of COVID-19 [64–68]. However, while the minimalistic SIR model offers some advantages, such as numerical efficiency and overseeable general conclusions, very few underlying assumptions, and accessibility for upgrades, it also has some drawbacks. With this phenomenological approach we do not account for behavioral adaptations, age stratification, and for the multiple disease processes that are characteristic for the new coronavirus disease, such as the latent phase, asymptomatic infections, deaths, and reoccurring infections. These are important features to consider when developing realistic COVID-19 epidemiological models and models designed to predict future epidemic trajectories [69–72], which, however, goes beyond the scope of the present study. Nevertheless, it should be emphasized that the main findings of our phenomenological model match with some recent studies aimed to investigate more explicitly the impact of travel restrictions on the progression of COVID-19. Specifically, it has been demonstrated that travel bans do not appear to have a long term impact on the spreading of the disease unless the transportation between regions is completely locked down, which is mostly not feasible for both practical and economic reasons [73, 74]. Along similar lines, other data-driven approaches that considered the spatial spread of the disease have also shown that reducing the flow of individuals is not a very effective strategy if not accompanied by other containment measures, in particular early case identification and isolation [62].

At the time of writing, we are facing a truly global epidemic, with many millions infected with COVID-19 around the world, while having all these insights about how and why epidemics spread [1, 2], and how best to contain them—at least in theory. This is largely due to seminal advances in network science, which together with complex systems science and methods of applied mathematics and statistical physics have provided insights that we simply did not have before. Unfortunately, however, the media landscape is rapidly changing too, with fake news and misinformation frequently taking over the narrative [75, 76], and leading astray reason and sound advice. The goal certainly is to move away from rather crude and almost ancient measures, and to encourage self-restrain and social responsibility through research. We certainly have the knowledge to halt epidemic spreading, at least to the point where it becomes humanly manageable without tsunamis of infected individuals pouring into overcrowded hospitals that are run by overexerted staff.

Many recent in-depth empirical and data-driven studies have investigated the effectiveness of different government interventions against COVID-19 [59, 60, 62]. It has been argued that many of the very restrictive containment strategies, such as stay-at-home orders, have a non-significant beneficial effect when compared to other less restrictive interventions. Considering the harmful health effects of very repressive measures and the possibility of their many counter-productive effects, it seems therefore crucial to target only the key determinants that affect the case growth rates. In parallel, it is important to raise awareness of the disease risk among the population, as it has been identified as a very strong driver of anti-contagion behavior [63, 77]. This is associated with collective intelligence and the willingness to cooperate [31, 39]—to take away from our own wellbeing and comfort to benefit others—to do without such measures.

Notably, the very same social dilemma—a situation where our own interests are at odds with what is best for the society as a whole—awaits when time comes to take a vaccine against an infectious disease [32]. And in this case too there is much we can look back on that has been discovered in the past decade in terms of better understanding and implementing a successful and efficient vaccination program [35].

Future research should look more closely into the relevance and potential impact of higher-order interactions, i.e. social networks where a single link connects more than just two individuals [78]. Recent research has shown that this alteration in the way we model our interactions can have important consequences for social contagion, honesty, and cooperation [79, 80]. And there is good reason to explore models of epidemic spreading on higher-order social networks in great detail, since we live and thrive in collectives like few other species. This collectiveness continues to be a key pillar that facilitates our societal and technological progress, but it may also be an important factor that facilitates the spread of epidemics.

We hope that this research will help pave the way towards more effective measures, as far as this is possible, to stem the burden of mitigating epidemic spreading. We are reminded time and again throughout history that epidemics are recurrent, and that we thus have to remain vigilant and armed with the best knowledge attainable to arrest them successfully.

Acknowledgments

We gratefully acknowledge funding from the Slovenian Research Agency (Grant Nos. P1-0403, J1-2457, P3-0396, P1-0055, and I0-0029).

Data availability statement

All data that support the findings of this study are included within the article (and any supplementary files).

ORCID iDs

Marko Gosak https://orcid.org/0000-0001-9735-0485
Matjaž Perc https://orcid.org/0000-0002-3087-541X

References

[1] Pastor-Satorras R, Castellano C, Van Mieghem P and Vespignani A 2015 *Rev. Mod. Phys.* **87** 925–79
[2] de Arruda G F, Rodrigues F A and Moreno Y 2018 *Phys. Rep.* **756** 1–59
[3] Watts D J and Strogatz S H 1998 *Nature* **393** 440–2
[4] Barabási A-L and Albert R 1999 *Science* **286** 509–12
[5] Pastor-Satorras R and Vespignani A 2001 *Phys. Rev. Lett.* **86** 3200
[6] Moreno Y, Pastor-Satorras R and Vespignani A 2002 *Eur. Phys. J.* B **26** 521–9
[7] Lagorio C, Dickison M, Vazquez F, Braunstein L A, Macri P A, Migueles M, Havlin S and Stanley H E 2011 *Phys. Rev.* E **83** 026102
[8] Rocha L E C, Liljeros F and Holme P 2011 *PLoS Comput. Biol.* **7** e1001109
[9] Takaguchi T, Masuda N and Holme P 2013 *PLoS One* **8** e68629
[10] Brockmann D and Helbing D 2013 *Science* **342** 1337–42
[11] Saad-Roy C M, Wingreen N S, Levin S A and Grenfell B T 2020 *Proc. Natl Acad. Sci. USA* **117** 11541–50
[12] Masuda N and Holme P 2017 *Temporal Network Epidemiology* (New York: Springer)
[13] González M C, Hidalgo C A and Barabási A-L 2008 *Nature* **453** 779–82
[14] Meloni S, Arenas A and Moreno Y 2009 *Proc. Natl Acad. Sci.* **106** 16897–902
[15] Belik V, Geisel T and Brockmann D 2011 *Phys. Rev.* X **1** 011001
[16] Kraemer M U G *et al* 2020 *Science* **368** 493–7
[17] Hâncean M-G, Perc M and Lerner J 2020 *R. Soc. Open Sci.* **7** 200780
[18] Aleta A *et al* 2020 *Nat. Hum. Behav.* **4** 964–71
[19] Bonaccorsi G *et al* 2020 *Proc. Natl Acad. Sci. USA* **117** 15530–5
[20] Chang S, Pierson E, Koh P W, Gerardin J, Redbird B, Grusky D and Leskovec J 2020 *Nature* **589** 82–7
[21] Girvan M and Newman M E J 2002 *Proc. Natl Acad. Sci.* **99** 7821–6
[22] Liu Z and Hu B 2005 *Europhys. Lett.* **72** 315–21
[23] Nematzadeh A, Ferrara E, Flammini A and Ahn Y Y 2014 *Phys. Rev. Lett.* **113** 088701
[24] Stegehuis C, van der Hofstad R and van Leeuwaarden J S H 2016 *Sci. Rep.* **6** 29748
[25] Nadini M, Sun K, Ubaldi E, Starnini M, Rizzo A and Perra N 2018 *Sci. Rep.* **8** 2352
[26] Valdez L D, Braunstein L A and Havlin S 2020 *Phys. Rev.* E **101** 032309
[27] Salathé M and Jones J H 2010 *PLoS Comput. Biol.* **6** e1000736
[28] Christakis N A and Fowler J H 2009 *Connected: the Surprising Power of Our Social Networks and How They Shape Our Lives* (New York: Little Brown)
[29] Easley D and Kleinberg J 2010 *Networks, Crowds, and Markets* (Cambridge: Cambridge University Press)
[30] Reluga T C 2010 *PLoS Comput. Biol.* **6** e1000793
[31] Bavel J J V *et al* 2020 *Nat. Hum. Behav.* **4** 460–71
[32] Bauch C T and Earn D J D 2004 *Proc. Natl Acad. Sci.* **101** 13391–4
[33] Fu F, Rosenbloom D I, Wang L and Nowak M A 2011 *Proc. R. Soc. B.* **278** 42–9
[34] Chen X and Fu F 2019 *Proc. R. Soc. B.* **286** 20182406
[35] Wang Z, Bauch C T, Bhattacharyya S, d'Onofrio A, Manfredi P, Perc M, Perra N, Salathé M and Zhao D 2016 *Phys. Rep.* **664** 1–113
[36] Nowak M A and Highfield R 2011 *SuperCooperators: Altruism, Evolution, and Why We Need Each Other to Succeed* (New York: Free Press)
[37] Rand D G and Nowak M A 2013 *Trends Cogn. Sci.* **17** 413–25
[38] Perc M, Jordan J J, Rand D G, Wang Z, Boccaletti S and Szolnoki A 2017 *Phys. Rep.* **687** 1–51
[39] Levin S A 2020 *Unsolved Problems in Ecology* ed G D Tilman, R D Holt and A Dobson (Princeton: Princeton University Press) p 311
[40] Dong E, Du H and Gardner L 2020 *Lancet Infect. Dis.* **20** 533–4
[41] Maier B F and Brockmann D 2020 *Science* **368** 742–6
[42] Priesemann V *et al* 2021 *Lancet* **397** 92–3
[43] Priesemann V *et al* 2021 *Lancet* **397** 469–70
[44] Schippers M C 2020 *Front. Psychol.* **11** 2626
[45] Boguná M, Papadopoulos F and Krioukov D 2010 *Nat. Commun.* **1** 62
[46] Krioukov D, Papadopoulos F, Kitsak M, Vahdat A and Boguná M 2010 *Phys. Rev.* E **82** 036106
[47] Zuev K, Boguná M, Bianconi G and Krioukov D 2015 *Sci. Rep.* **5** 9421
[48] Duh M, Gosak M and Perc M 2021 *Chaos Solitons Fractals* **144** 110720

[49] Papadopoulos F, Kitsak M, Serrano M Á, Boguñá M and Krioukov D 2012 *Nature* **489** 537–40
[50] Wu Z, Di Z and Fan Y 2020 *Complexity* **2020** 8372928
[51] Humphries M D and Gurney K 2008 *PloS One* **3** e0002051
[52] Kleineberg K K 2017 *Nat. Commun.* **8** 1888
[53] Gosak M, Kraemer M U G, Nax H H, Perc M and Pradelski B S R 2021 *Sci. Rep.* **11** 3093
[54] Cho E, Myers S A and Leskovec J 2011 Friendship and mobility: user movement in location-based social networks *Proc. of the 17th ACM SIGKDD Int. Conf. on Knowledge discovery and Data Mining (ACM)* pp 1082–90
[55] Newman M E and Girvan M 2004 *Phys. Rev.* E **69** 026113
[56] Fortunato S 2010 *Phys. Rep.* **486** 75–174
[57] Binder K and Hermann D K 1988 *Monte Carlo Simulations in Statistical Physics* (Heidelberg: Springer)
[58] Enright J and Kao R R 2018 *Epidemics* **24** 88–97
[59] Brauner J M *et al* 2021 *Science* **371** eabd9338
[60] Perra N 2021 *Phys. Rep.* (in press) https://doi.org/10.1016/j.physrep.2021.02.001
[61] Lai S *et al* 2020 *Nature* **585** 410–3
[62] Aleta A and Moreno Y 2020 *BMC Med.* **18** 157
[63] Bendavid E, Oh C, Bhattacharya J and Ioannidis J P A 2021 *Eur. J. Clin. Invest.* **51** e13484
[64] Abou-Ismail A 2020 *SN Compr. Clin. Med.* **2** 852–8
[65] Law K B *et al* 2020 *Sci. Rep.* **10** 21721
[66] Cooper I, Mondal A and Antonopoulos C G 2020 *Chaos Solitons Fractals* **139** 110057
[67] Roda W C, Varughese M B, Han D and Li M Y 2020 *Infect. Dis. Model.* **5** 271–81
[68] Kudryashov N A, Chmykhov M A and Vigdorowitsch M 2021 *Appl. Math. Model.* **90** 466–73
[69] Moein S, Nickaeen N, Roointan A, Borhani N, Heidary Z, Javanmard S H, Ghaisari J and Gheisari Y 2021 *Sci. Rep.* **11** 4725
[70] Amaral M A, Oliveira M M d and Javarone M A 2021 *Chaos Solitons Fractals* **143** 110616
[71] Ngonghala C N, Iboi E, Eikenberry S, Scotch M, MacIntyre C R, Bonds M H and Gumel A B 2020 *Math. Biosci.* **325** 108364
[72] Firth J A, Hellewell J, Klepac P, Kissler S, Kucharski A J and Spurgin L G 2020 *Nat. Med.* **26** 1616–22
[73] Aleta A, Hu Q, Ye J, Ji P and Moreno Y 2020 *Chaos Solitons Fractals* **139** 110068
[74] Kuzdeuov A, Baimukashev D, Karabay A, Ibragimov B, Mirzakhmetov A, Nurpeiissov M, Lewis M and Varol H A 2020 *IEEE J. Biomed. Health Inform.* **24** 2743–54
[75] Del Vicario M, Bessi A, Zollo F, Petroni F, Scala A, Caldarelli G, Stanley H E and Quattrociocchi W 2016 *Proc. Natl Acad. Sci. USA* **113** 554–9
[76] Cinelli M, Quattrociocchi W, Galeazzi A, Valensise C M, Brugnoli E, Schmidt A L, Zola P, Zollo F and Scala A 2020 arXiv: 2003.05004
[77] Travaglino G A and Moon C 2021 *Front. Psychol.* **12** 684
[78] Battiston F, Cencetti G, Iacopini I, Latora V, Lucas M, Patania A, Young J-G and Petri G 2020 *Phys. Rep.* **874** 1–92
[79] de Arruda G F, Petri G and Moreno Y 2020 *Phys. Rev. Res.* **2** 023032
[80] Alvarez-Rodriguez U, Battiston F, de Arruda G F, Moreno Y, Perc M and Latora V 2020 *Nat. Hum. Behav.* 1–9